



# Constructing metamaterials from subwavelength pixels with constant indices product

Jensen Li, Feng Miao, Zixian Liang, Sebastien Guenneau

## ► To cite this version:

Jensen Li, Feng Miao, Zixian Liang, Sebastien Guenneau. Constructing metamaterials from subwavelength pixels with constant indices product. Optics Express, 2015, 23, pp.7140-7151. 10.1364/OE.23.007140 . hal-01217462

**HAL Id: hal-01217462**

**<https://amu.hal.science/hal-01217462>**

Submitted on 19 Oct 2015

**HAL** is a multi-disciplinary open access archive for the deposit and dissemination of scientific research documents, whether they are published or not. The documents may come from teaching and research institutions in France or abroad, or from public or private research centers.

L'archive ouverte pluridisciplinaire **HAL**, est destinée au dépôt et à la diffusion de documents scientifiques de niveau recherche, publiés ou non, émanant des établissements d'enseignement et de recherche français ou étrangers, des laboratoires publics ou privés.

# Constructing metamaterials from subwavelength pixels with constant indices product

Jensen Li,<sup>1,3\*</sup> Feng Miao,<sup>2</sup> Zixian Liang<sup>2,3</sup> and Sebastien Guenneau<sup>4,5</sup>

<sup>1</sup>*School of Physics and Astronomy, University of Birmingham, Birmingham B15 2TT, UK*

<sup>2</sup>*Department of Physics and Materials Science, City University of Hong Kong, Kowloon Tong, Hong Kong, China*

<sup>3</sup>*Shenzhen Research Institute, City University of Hong Kong, Shenzhen, China*

<sup>4</sup>*Aix-Marseille Université, CNRS, Ecole Centrale Marseille, Institut Fresnel, Campus Universitaire de Saint-Jérôme, Marseille, F-13013, France*

<sup>5</sup>*sebastien.guenneau@fresnel.fr  
j.li@bham.ac.uk*

**Abstract.** We investigate a two-dimensional metamaterial template constructed from different pixels through a conservation law of effective indices: If the product of refractive indices along the principal axes is invariant for different anisotropic materials in a two-dimensional space, the product of indices of the effective medium remains constant after mixing these materials. Such effective media of constant indices product can be implemented using metamaterial structures. The orientation of the metamaterial structure in a single pixel controls the direction of the principal axis of the effective medium. Different pixels are assembled into an array to obtain reconfigurable anisotropy of the effective medium. These considerations would be useful for constructing reconfigurable metamaterials and transformation media with area-preserving maps.

©2015 Optical Society of America

**OCIS codes:** (160.3918) Metamaterials; (260.2110) Electromagnetic optics; (310.6860) Thin films, optical properties.

---

## References and links

1. D. R. Smith, J. B. Pendry, and M. C. K. Wiltshire, "Metamaterials and Negative Refractive Index," *Science* **305**(5685), 788–792 (2004).
2. J. C. Maxwell Garnett, "Colours in Metal Glasses and in Metallic Films," *Philos. Trans. R. Soc. Lond. B Biol. Sci.* **203**(359-371), 385–420 (1904).
3. D. A. G. Bruggeman, "Berechnung verschiedener physikalischer Konstanten von heterogenen Substanzen. I. Dielektrizitätskonstanten und Leitfähigkeiten der Mischkörper aus isotropen Substanzen," *Annalen. Der. Physik.* **24**(7), 636–664 (1935).
4. D. Polder and J. H. Van Santen, "The effective permeability of mixtures of solids," *Physica* **12**(5), 257–271 (1946).
5. G. P. de Loor, "Dielectric properties of heterogeneous mixtures with a polar constituent," *Appl. Sci. Res. B.* **11**(3-4), 310–320 (1964).
6. H. Looyenga, "Dielectric constants of heterogeneous mixtures," *Physica* **31**(3), 401–406 (1965).
7. A. H. Sihvola and J. A. Kong, "Effective permittivity of dielectric mixtures," *IEEE Trans. Geosci. Rem. Sens.* **26**(4), 420–429 (1988).
8. D. J. Bergman, "Exactly Solvable Microscopic Geometries and Rigorous Bounds for the Complex Dielectric Constant of a Two-Component Composite Material," *Phys. Rev. Lett.* **44**(19), 1285–1287 (1980).
9. G. Nguetseng, "A general convergence result for a functional related to the theory of homogenization," *SIAM J. Math. Anal.* **20**(3), 608–623 (1989).
10. G. Allaire, "Homogenization and two-scale convergence," *SIAM J. Math. Anal.* **23**(6), 1482–1518 (1992).
11. S. Guenneau and F. Zolla, "Homogenization of Three-Dimensional Finite Photonic Crystals," *Progress In Electromagnetic Research.* **27**, 91–127 (2000).
12. N. Wellander and G. Kristensson, "Homogenization of the Maxwell Equations at Fixed Frequency," *SIAM. J. Math.* **64**, 170 (2003).
13. V. Jikov, S. Kozlov, and O. Oleinik, *Homogenization of Differential Operators* (Springer-Verlag, 1995).
14. G. W. Milton, *The theory of composites*, Cambridge University Press, Cambridge (2002).
15. B. Vasic, G. Isic, R. Gajic, and K. Hingerl, "Coordinate transformation based design of confined metamaterial structures," *Phys. Rev. B* **79**(8), 085103 (2009).
16. T. C. Han, C. W. Qiu, J. W. Dong, X. H. Tang, and S. Zouhdi, "Homogeneous and isotropic bends to tunnel

- waves through multiple different/equal waveguides along arbitrary directions,” *Opt. Express* **19**(14), 13020–13030 (2011).
17. Z. Liang, X. Jiang, F. Miao, S. Guenneau, and J. Li, “Transformation media with variable optical axes,” *New J. Phys.* **14**(10), 103042 (2012).
  18. H.-R. Wenk and P. Van Houtte, “Texture and anisotropy,” *Rep. Prog. Phys.* **67**(8), 1367–1428 (2004).
  19. L. Shi, P. F. McManamon, and P. J. Ros, “Liquid crystal optical phase plate with a variable in-plane gradient,” *J. Appl. Phys.* **104**(3), 033109 (2008).
  20. S. A. Ramakrishna, J. B. Pendry, M. C. K. Wiltshire, and W. J. Stewart, “Imaging the Near Field,” *J. Mod. Opt.* **50**(9), 1419–1430 (2003).
  21. A. Salandrino and N. Engheta, “Far-field subdiffraction optical microscopy using metamaterial crystals: Theory and simulations,” *Phys. Rev. B* **74**(7), 075103 (2006).
  22. H. Y. Chen and C. T. Chan, “Electromagnetic wave manipulation by layered systems using the transformation media concept,” *Phys. Rev. B* **78**(5), 054204 (2008).
  23. R. V. Craster and Y. V. Obnosov, “Four-Phase Checkerboard Composites,” *SIAM J. Appl. Math.* **61**(6), 1839–1856 (2001).
  24. R. V. Craster and Y. V. Obnosov, “Checkerboard composites with separated phases,” *J. Math. Phys.* **42**(11), 5379 (2001).
  25. G. W. Milton, “Proof of a conjecture on the conductivity of checkerboards,” *J. Math. Phys.* **42**(10), 4873 (2001).
  26. F. Zolla and S. Guenneau, “Duality relation for the Maxwell system,” *Phys. Rev. E Stat. Nonlin. Soft Matter Phys.* **67**(2 Pt 2), 026610 (2003).
  27. S. Chakrabarti, S. A. Ramakrishna, and S. Guenneau, “Finite checkerboards of dissipative negative refractive index,” *Opt. Express* **14**(26), 12950–12957 (2006).
  28. C. Della Giovampaola and N. Engheta, “Digital metamaterials,” *Nat. Mater.* **13**(12), 1115–1121 (2014).
  29. A. Castanié, J.-F. Mercier, S. Félix, and A. Maurel, “Generalized method for retrieving effective parameters of anisotropic metamaterials,” *Opt. Express* **22**(24), 29937–29953 (2014).
  30. R. Schittny, M. Kadic, S. Guenneau, and M. Wegener, “Experiments on Transformation Thermodynamics: Molding the Flow of Heat,” *Phys. Rev. Lett.* **110**(19), 195901 (2013).
  31. S. Guenneau and J. Li, “Conservation law in anisotropic effective thin plates” (in preparation)
  32. J. D. Jackson, *Classical Electrodynamics*, 3rd ed. (John Wiley & Sons, 1999).

## 1. Introduction

Homogenization of composite materials is an important topic in optics for understanding wave propagation and is currently with a renewed interest due to the developments of metamaterials [1]. It provides us with a macroscopic description of a composite material and is therefore useful for predicting and modeling complex wave phenomena when different composite materials are used as building blocks. In the long wavelength limit for dielectric composites, Maxwell Garnett (MG) formula deals with spherical inclusions embedded in a host material. Bruggeman's model works well when the two constituents are intermingled with each other [2,3]. In fact, different effective medium formulas have to be used for calculating the effective material parameters in different situations [4–7]. There are also approaches focusing on more general aspects of homogenization. For example, the Bergman-Milton theory can be used for deriving rigorous bounds for the effective material parameters consisting of two isotropic dielectric media with complex relative permittivities: Based on very general physical principles, these rigorous bounds confine the region of the physically admissible effective permittivities in the complex plane [8]. Two-scale convergence has been developed to obtain the effective material parameters which can capture all interaction effects between the inclusions [9,10]. The refined homogenization results for the Maxwell system [11,12] encompass the cases of small and large volume fraction and regular as well as irregular shapes of inclusions and can be applied in more general contexts [13,14]. We note that classical effective medium theories are often isotropic for both the constituting materials and the resultant effective medium due to random fluctuations. However, with the availability of metamaterials whose refractive indices and local anisotropy can be precisely controlled with varying profiles, the consideration of effective media with artificial anisotropy becomes increasingly important.

In this paper, we first point out a mixing law for anisotropic effective medium theory in which the product of principal indices of an effective medium remains constant throughout the homogenization process with specific conditions. In this law, the constant property of mixture is independent of the filling ratio and is also independent of the shape of material

inclusions (established through two-scale convergence), which is guaranteed in the long wavelength limit. With the help of this law, we can extend the application of homogenization to a class of anisotropic effective media with constant indices product which can be potentially useful for designing reconfigurable two-dimensional metamaterials and transformation optical (TO) media associated with area-preserving mappings [15–17].

The paper is organized in the following way. Section 1 is the present introduction. In section 2, we introduce the conservation law about the indices product that we employ in this work as a way to construct metamaterial templates. In section 3, we numerically demonstrate the conservation law by considering an array of cylinders with anisotropic permittivities. In section 4, we propose a reconfigurable effective medium with constant indices product, which can be tuned by rotating a metamaterial atom. In section 5, we use the individually reconfigurable pixels developed in section 4 to construct higher order effective media (super lattice) of constant indices product using a bilayer structure and a checkerboard structure, as a route to a reconfigurable metamaterial template. Section 6 is the summary of this work.

## 2. Index conservation for anisotropic effective media

We begin by specifying an arbitrary profile of anisotropic permittivity tensor  $\epsilon(\mathbf{r})$  on the micro-scale, satisfying the usual assumption of homogenization theory (uniform and strictly positive upper and lower bounds for almost every position vector  $\mathbf{r}$  in a periodic cell, what covers the case of piecewise constant periodic permittivity functions) [9–13]. It is well known that the homogenization problem amounts to solving a local problem in a periodic cell with a constant electric field  $\mathbf{E}_0$  applied to the system shown in Fig. 1.

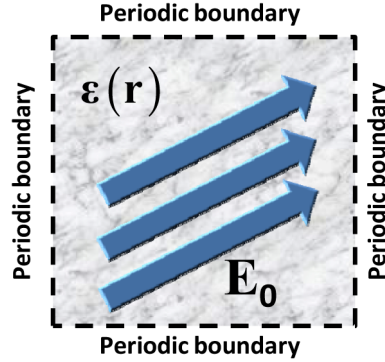


Fig. 1. The local annex problem obtained from the homogenization process in a 2D periodic structure with a square unit cell. Permittivity  $\epsilon(\mathbf{r})$  denotes distribution of materials in the domain. Arrows  $\mathbf{E}_0$  represent the constant electric field applied to the background. Periodic boundary conditions are applied.

The local problem obtained from the homogenization of periodic dielectric media (two-scale convergence) [11–14] corresponds to solving the Laplace equation

$$\nabla \cdot (\epsilon(\mathbf{r}) \cdot \mathbf{E}(\mathbf{r})) = 0, \quad (1)$$

with  $\mathbf{E}(\mathbf{r})$  being the electric field such that

$$\begin{aligned} \mathbf{E}(\mathbf{r}) &= \langle \mathbf{E} \rangle - \nabla V(\mathbf{r}) \\ \mathbf{D}(\mathbf{r}) &= \langle \mathbf{D} \rangle + \nabla \times \mathbf{U}(\mathbf{r}) \\ \mathbf{D}(\mathbf{r}) &= \epsilon(\mathbf{r}) \cdot \mathbf{E}(\mathbf{r}) \end{aligned} \quad (2)$$

where  $\mathbf{U}(\mathbf{r})$  and  $V(\mathbf{r})$  are vector and scalar potentials, respectively. Equation (1) is solved subject to periodic boundary conditions on the square domain shown in Fig. 1.  $\mathbf{E}_0$  is the constant applied external electric field, which is also the (spatially) averaged E-field  $\langle \mathbf{E} \rangle$  in the current work due to the periodicity of  $V(\mathbf{r})$ . The effective medium is then obtained from the averaged fields as

$$\langle \mathbf{D} \rangle = \langle \boldsymbol{\varepsilon} \cdot \mathbf{E} \rangle = \boldsymbol{\varepsilon}_{\text{eff}} \cdot \langle \mathbf{E} \rangle. \quad (3)$$

By integrating  $\int d^2r V_a$  on  $\nabla \cdot \mathbf{D}_b = 0$  with periodic boundary condition and using the  $\nabla V$  in Eq. (2), we obtain

$$\langle \mathbf{E}_a \cdot \mathbf{D}_b \rangle = \langle \mathbf{E}_a \rangle \cdot \langle \mathbf{D}_b \rangle, \quad (4)$$

where the subscripts  $a$  and  $b$  indicate two sets of solutions (with applied external electric field  $\mathbf{E}_{0a}$  and  $\mathbf{E}_{0b}$ ). One notes that  $\boldsymbol{\varepsilon}^{\text{eff}}$  is symmetric from the assumption of symmetric local  $\boldsymbol{\varepsilon}$  at every point:

$$\langle \mathbf{E}_a \rangle \cdot \boldsymbol{\varepsilon}^{\text{eff}} \langle \mathbf{E}_b \rangle = \langle \mathbf{E}_a \cdot \boldsymbol{\varepsilon} \cdot \mathbf{E}_b \rangle = \langle \mathbf{E}_b \rangle \cdot \boldsymbol{\varepsilon}^{\text{eff}} \langle \mathbf{E}_a \rangle. \quad (5)$$

For a two-dimensional problem, all the vector fields  $\mathbf{E}$  and  $\mathbf{D}$  stay in-plane,  $\mathbf{E}$ ,  $\mathbf{D}$ ,  $V$  and the 2x2 permittivity tensor  $\boldsymbol{\varepsilon}$  are invariant along  $z$  axis. We can similarly obtain (through integration-by-parts with  $\int d^3r V_a \nabla \times \mathbf{E}_b$  and  $\int d^3r \hat{z} \cdot \mathbf{U}_a \nabla \cdot \mathbf{D}_b$ ):

$$\begin{aligned} \langle \mathbf{E}_a \times \mathbf{E}_b \rangle &= \langle \mathbf{E}_a \rangle \times \langle \mathbf{E}_b \rangle \\ \langle \hat{z} \cdot \mathbf{D}_a \times \mathbf{D}_b \rangle &= \hat{z} \cdot \langle \mathbf{D}_a \rangle \times \langle \mathbf{D}_b \rangle. \end{aligned} \quad (6)$$

Then, we can derive the following identity:

$$\begin{aligned} \langle \hat{z} \cdot \mathbf{E}_a \times \mathbf{E}_b \det \boldsymbol{\varepsilon} \rangle &= \langle \hat{z} \cdot \mathbf{D}_a \times \mathbf{D}_b \rangle \\ &= \hat{z} \cdot \langle \mathbf{D}_a \rangle \times \langle \mathbf{D}_b \rangle = \hat{z} \cdot \langle \mathbf{E}_a \rangle \times \langle \mathbf{E}_b \rangle \det \boldsymbol{\varepsilon}^{\text{eff}} \\ &= \langle \hat{z} \cdot \mathbf{E}_a \times \mathbf{E}_b \rangle \det \boldsymbol{\varepsilon}^{\text{eff}}. \end{aligned} \quad (7)$$

Now, if  $\det \boldsymbol{\varepsilon}$  does not depend on position, a condition which we impose on all the materials, we have

$$\det \boldsymbol{\varepsilon}^{\text{eff}} = \det \boldsymbol{\varepsilon} \text{ if } \det \boldsymbol{\varepsilon} = \text{constant}. \quad (8)$$

This serves as our basic principle, being called the “index conservation law” in this work, to be used in constructing reconfigurable metamaterials and transformation media in the following sections. The determinant in Eq. (8) ensures that if the product of the refractive indices along the two principal axes is a constant independent of position before mixing, the effective medium keeps the same product of indices along the two final principal axes. It is actually a more general result than what we have previously used in [17], in which we stated that by mixing the same kind of anisotropic material, also for textured polycrystals (e.g. calcite rock) and liquid crystals [18,19], with different orientations, the product of principal refractive indices of the effective medium stays the same. We have to note that the results here are only valid for two dimensional effective media (without a straight-forward correspondence in three dimensional case) where both materials and fields are invariant in the third dimension. On the other hand, we can consider specific kinds of two-dimensional effective media in which analytic formulas can be derived and verified to satisfy the

conservation law, including a case of anisotropic cylinders in an isotropic matrix and another case of stratified anisotropic layers listed in the Appendix.

### 3. Numerical validation of the index conservation law

To illustrate the index conservation law before discussing its application, we first consider a square array of cylinders, as shown in inset of Fig. 2. The lattice constant is chosen as 1 without losing generality and the radius of the cylinder is 0.3. The arrows (with the elliptical equipfrequency contour) denote the direction of optical axis  $\hat{\alpha}$  with  $n_\alpha < n_\beta$ , making an angle  $\theta$  to the x-axis. The other optical axis  $\hat{\beta}$  normal to  $\hat{\alpha}$  is not plotted here. The principal refractive indices are defined as  $n_\alpha = \sqrt{\epsilon_\beta}$  and  $n_\beta = \sqrt{\epsilon_\alpha}$  and the anisotropy factor  $\gamma$  is defined as the ratio between the larger and smaller principal indices ( $\gamma = n_\beta/n_\alpha$ ) so that we can use  $(\gamma, \hat{\alpha})$  to describe the anisotropic constituents completely with the subscript  $I = s$  for the matrix domain and  $I = c$  for the cylindrical domain. As an example, we set the background anisotropic permittivity as  $(\epsilon_\alpha^s, \epsilon_\beta^s) = (5/2, 8/5)$  and of the cylinder as  $(\epsilon_\alpha^c, \epsilon_\beta^c) = (4, 1)$ . The anisotropies in the two domains  $\gamma_s = 1.25$  and  $\gamma_c = 2$  are different while the determinant of the individual permittivity tensor  $\epsilon_\alpha \epsilon_\beta$  is kept at the same constant 4 so that the index conservation law can be utilized.

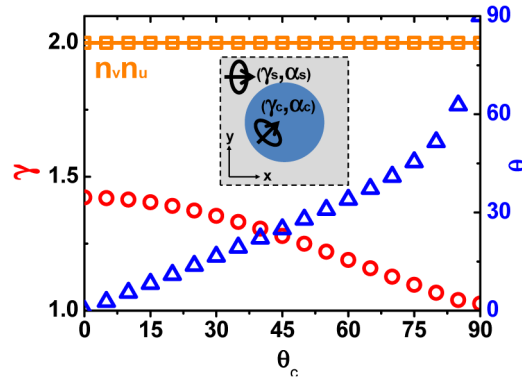


Fig. 2. Homogenization of effective media for a square array of circular inclusions (parameters described in text). Inset is the sketch of mixture. Elliptical equipfrequency contours denote anisotropy in different domains and arrows indicate individual directions of optical axis.

Next we calculate the averaged displacement  $\mathbf{D}$  induced by a constant external field  $\mathbf{E}_0$  with finite element analysis (COMSOL Multiphysics, electrostatics module) with periodic boundary condition on the square unit cell. We can get the effective permittivity tensor  $\epsilon^{eff}$  by doing two simulations (two elements from each simulation with external field either in the x- or y-direction) and using the definition in Eq. (3). The effective principal axis indices  $(n_v, n_u)$  is then obtained by finding the eigenvalue of  $\epsilon^{eff}$  and the effective direction of optical axis  $\theta$  is related to its eigenvectors (here  $v$  and  $u$  are the new directions of principal optical axes). We define the effective anisotropy  $\gamma$  as  $n_v/n_u$  with  $n_v > n_u$ . In Fig. 2, we change  $\hat{\alpha}_c$  (optical axis of the medium in circular inclusion) continuously from 0 to  $\pi/2$  with a fixed  $\hat{\alpha}_s$  (optical axis of the medium in square area) at angle 0 and calculate the effective indices  $n_v$  and  $n_u$ . The numerical result shows complete consistency with the index conservation law in Eq. (8). We can see the discrete symbols in orange color (simulation

results) reveal the fact that the product of effective principal indices is a constant which is denoted by a solid line (expected result from Eq. (8)) against different directions of optical axis  $\theta_c$ . In addition, Fig. 2 also indicates that we can have a medium with constant  $n_v n_u$  but a tunable effective anisotropy and also the direction of resultant principal axes by rotating the local optical axis of the cylinder. We have shown a specific case of square array of cylinders in a matrix material while the index conservation law is also valid for other geometries and for more than two material domains as long as the principal indices product for all material domains are the same constant.

#### 4. Reconfigurable effective medium with constant principal indices product using metamaterial structures

The index conservation law points to the possibility of a reconfigurable effective medium through rotating local optical axes (of the core cylinder of the previous example). Here, we implement such an effective medium with constant indices product by using an anisotropic metamaterial atom. The scheme is shown in Fig. 3. Structure *a1* contains an anisotropic homogenous medium (*c*) with a circular disk geometry. It is to be replaced by structure *a2*, which we choose to be a pair of metal bars (made of perfect conductors) embedded in air (*c'*) with the same circular boundary. After an effective medium equivalence between structure *a1* and *a2* is drawn, we further embed a square array of these homogeneous anisotropic cylinders or metal bars in an isotropic background dielectric medium. Now, we can choose a background medium (*s*) to have the same index product as the core cylinder. According to the index conservation law, the same index product is carried to the effective medium of the whole structure. Rotating the metamaterial atom (*c'*) is equivalent to rotating the optical axis of *c*. It keeps the index product invariant while the effective optical axis and effective anisotropy factor may then be tuned.

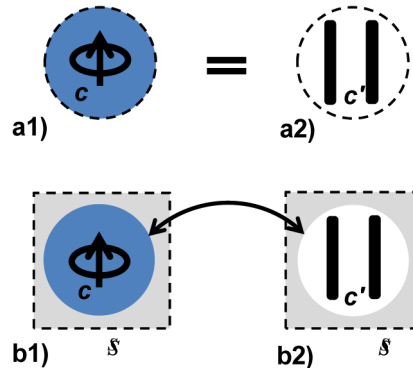


Fig. 3. A reconfigurable effective medium implemented by metamaterial atoms. Structure *a1* denotes the homogeneous anisotropic media *c* with a circular disk geometry, which can be considered as the effective media of the circular disk structure *a2* which is composed by air *c'* of the same size with double perfect electric conductor (PEC) bars inside. Structures *b1* and *b2* are the corresponding structures embedded in an isotropic background in matching the principal indices product.

As an example, we set the length, width and distance between the bars to be 0.7, 0.05 and 0.2, respectively. Lattice constant is 1 and the filling fraction of *c* or *c'* is set as 0.5. In practice, we do the above procedure in the reverse order. We find the effective medium of structure *b2* directly (with periodic boundary condition on the square unit cell) with increasing  $\epsilon^s$  (isotropic permittivity of background to be chosen) from 1 until reaching the target value such that the product of the principal indices of the whole effective medium is the

same as the one of background ( $\epsilon^s$ ). We found that to be  $\epsilon^s = 2.53$ . The corresponding product of principal indices of the effective medium against the orientation of the metal bars is plotted as square symbols in Fig. 4a, which agrees very well with the expected constant (2.53) except for some small discrepancies which can be attributed to the near-fields created by the metal bars. The product of the principal indices of the cylinder  $c$  is thus determined to be 2.53. The remaining anisotropy factor for the cylinder  $c$  can then be determined by matching the effective anisotropy factor of structure  $b1$  to the effective anisotropy factor  $\gamma_{b2}^{eff} = 1.445$  from simulating structure  $b2$  with the determined  $\epsilon^s$ . It yields the result  $\{\epsilon_x^c, \epsilon_y^c\} = \{5.42, 1.18\}$  before rotating the bars. From this point onwards, we can regard this to be the effective permittivity of the double bars inside the circular disk of air. We can then plot also the effective anisotropy and the effective orientation of structure  $b1$  and structure  $b2$  in Fig. 4 and they agree with each other very well. We will see more examples to confirm the obtained effective medium description of the double bars in the next section. In principle, we can also consider other shapes of inner domains, e.g. an ellipse or a square, so that the index conservation law is still valid and we can replace the inner domain to an anisotropic metamaterial atom in air. However, we choose a cylindrical inner domain here to maintain the rotational symmetry so that rotating the metamaterial atom (in structure  $b2$ ) means equivalently rotating the principal axis of the inner domain (in structure  $b1$ ), as the reconfigurability of the effective medium by rotation.

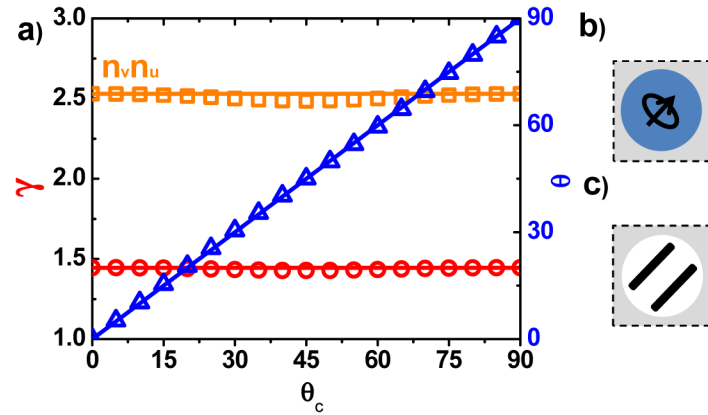


Fig. 4. Reconfigurable effective medium with microstructure in getting a constant index product. It is a pixel. The effective parameters are shown in a). Solid lines are for the homogenized model shown in b) while the discrete symbols are for the model with structures shown in c).  $\theta_c$  represents the rotation of optical axis of homogeneous medium in the disc as well as the rotation of the bars. Detailed dimensions are discussed in the text.

From Fig. 4, we have established a reconfigurable effective medium by rotating a metamaterial atom (double bars) for (nearly) constant indices product. The orientation of the final principal axes can be tuned by rotating the metamaterial atom. On the other hand, the anisotropy factor in the current case is in fact insensitive to the orientation of the metamaterial atom ( $c'$ ) or the homogeneous cylinder ( $c$ ) because we have employed an isotropic background (anisotropy is assumed from metamaterial atoms to be rotated) unlike the result in Fig. 2. We can in fact trace this angle insensitivity back to the Maxwell Garnett formula for such geometry in Appendix A. Now, we can regard the structure developed in this section as a basic pixel (with a rotatable metamaterial atom) in order to construct higher order effective medium with larger tunable range of anisotropy.



## 5. Reconfigurable effective media designed by double bars with super-lattices

With the principal axes of individual pixels able to be tuned by rotating the metamaterial atoms (double bars), we can construct a super-lattice with the atomic orientations. Figure 5 shows an example of stratified layer structure [20–22] with each layer (A or B) being one pixel in thickness. All the structural dimensions and material parameters are taken from the previous example. As both the cylinders region and background region (blue and gray color in Fig. 5(b)) have the same indices product, the super lattice has the same indices product, according to the index conservation law, as well. In layer A, we fix the optical axis along y direction and make the one tunable in layer B. The arrangement of optical axes is shown by the arrows in Fig. 5.b and it can be substituted by the double bars shown in Fig. 5(c). Now, we rotate the double bars in layer B, denoted as the variation of  $\theta_c$ . The effective medium results are shown in Fig. 5(a) in which discrete symbols represent the simulation results with the metamaterial double bars and solid lines represent the simulation results with the homogeneous cylinders. The two sets of result match each other very well, confirming our scheme in using the metamaterial atoms to construct the reconfigurable effective medium with constant indices product ( $n_v n_u$  is nearly a constant from the simulation results with microstructures). Both the effective anisotropy factor and the direction of the effective principal axes can be tuned by the orientations of the metamaterial atoms.

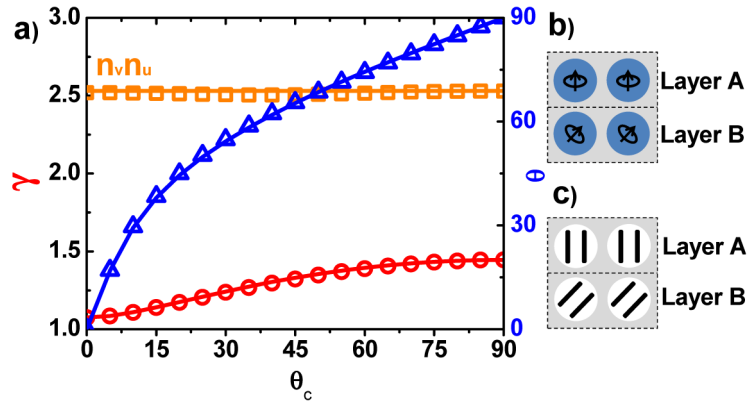


Fig. 5. Effective medium of constant indices product of a bilayer superlattice structure constructed from basic pixels in Fig. 4. Solid lines are results for the homogenized cylinder model shown in b). Discrete symbols are the results for the model with double bars shown in c).

Another example of super-structure is a checkerboard system (usually isotropic [23–27]). Here, we extend the application of checkerboard systems to an anisotropic case. It is shown in Fig. 6. We continue to make use of the same effective medium of the double bars system as a unit cell to construct the checkerboard in which the optical axis is fixed along x direction in pixel A and it is tunable in pixel B. Figure 6(b) is the system with homogeneous cylinder description while Fig. 6(c) is the one with microstructure for actual implementation. The constant line in Fig. 6(a) validates our law again with the solid lines denoting the homogenized cylinder model (Fig. 6(b)) while the discrete symbols denoting results for the double bars system model (Fig. 6(c)). Comparing to the bilayer superlattice, the checkerboard superlattice has a similar tunable range for the anisotropy factor while the direction of the effective principal axis can become a linear function of the orientation of the metamaterial atoms again for simplicity.

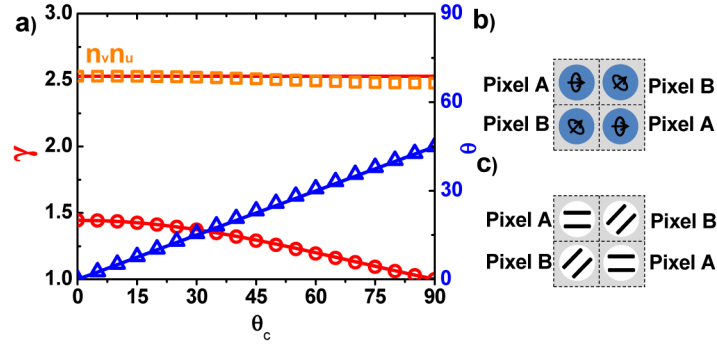


Fig. 6. Effective medium of constant indices product of a checkerboard superlattice structure constructed from basic pixels in Fig. 4. Solid lines are results for the homogenized model shown in b). Discrete symbols are the results for the model with double bars shown in c).

Both the bilayer and the checkerboard systems in the cases above show that we can find a general route to construct an effective medium for which the effective indices product  $n_v n_u$  is constant and the anisotropy can be tuned by rotating the structure. Although the numerical results show a small discrepancy (some fluctuation) between the homogenized cylinder and micro-structured models, this small discrepancy will not severely affect the final application in experiments. Although we have focused on using pixels with only a single degree of freedom about the orientation of the metamaterial structure, it is worthwhile to mention that the presented scheme can be further extended to pixels containing different anisotropy factors as long as the indices product is the same constant. This constant indices product is related to a transformation optical medium associated with an area-preserving map. Here, we are exploring a continuous degree of freedom from the orientation of the metamaterial structure in each pixel. We also note that there can be other different schemes. For example, one can also choose from two different isotropic permittivities in each pixel as a discrete degree of freedom for the reconfigurability of metamaterials [28].

## 6. Conclusion

In this work, by establishing an index conservation law in mixing anisotropic effective media of constant indices product, we can design reconfigurable effective media with microstructures composed of isotropic dielectrics and anisotropic metal bars. Importantly, the results presented in this paper hold for fixed frequency homogenization wherein the wavelength is much larger than the size of the periodic cell (in practice the wavelength to cell size ratio should be at least three). We note that apart from the two-scale convergence method used in this work, there are also other approaches based on scattering behavior in obtaining numerically the effective medium of anisotropic materials with generic settings [29]. One should also note that thanks to correspondences between electrostatic and certain elastostatic problems in heterogeneous cylindrical media, our law applies mutatis mutandis to the case of effective shear tensor for anti-plane shear waves in acoustic metamaterials. This law can also be applied to the effective tensor of conductivity for thermal metamaterials recently introduced in order to mould the flow of heat [30]. We are currently working on an extension of our law to flexural waves propagating in thin structured plates [31], and we hope to be able to find similar laws in hydrodynamics. In conclusion, we think this route is a step forward in operating and controlling propagation and diffusion phenomena in microstructured materials in the near future.

## Appendix A: Effective medium for an array of anisotropic circular cylinders in isotropic background

For an array of circular isotropic dielectric cylinders in a background isotropic dielectric medium, it is well known that the Maxwell Garnett (MG) formula gives the approximated effective permittivity when the filling fraction of the cylinders is small. It can be readily obtained from the Clausius-Mossotti equation in two dimensions with the single cylinder polarizability derived from the electrostatic problem when the cylinder is under a constant applied electric field [32]. As the electric field inside the cylinder is a constant and is along the same direction of the applied field, a variation of the permittivity of the cylinder in the direction perpendicular to the applied field does not change the field solution and hence the effective permittivity along the applied field direction is unchanged. It implies that the effective medium for a periodic array of anisotropic cylinders is decoupled in the two directions of principal axes. Suppose the permittivity tensor of the cylinder along the two principal axes is

$$\boldsymbol{\epsilon}^A = \begin{pmatrix} \epsilon_\alpha^A & 0 \\ 0 & \epsilon_\beta^A \end{pmatrix}. \quad (9)$$

and the permittivity of the isotropic background is  $\epsilon^B$ . Then the effective medium is governed by the MG formula:

$$\frac{\epsilon_\alpha^{\text{eff}} - \epsilon^B}{\epsilon_\alpha^{\text{eff}} + \epsilon^B} = f \frac{\epsilon_\alpha^A - \epsilon^B}{\epsilon_\alpha^A + \epsilon^B}. \quad (10)$$

and similarly

$$\frac{\epsilon_\beta^{\text{eff}} - \epsilon^B}{\epsilon_\beta^{\text{eff}} + \epsilon^B} = f \frac{\epsilon_\beta^A - \epsilon^B}{\epsilon_\beta^A + \epsilon^B}. \quad (11)$$

with zero off-diagonal terms in the effective permittivity tensor and  $f$  being the area filling fraction of the cylinders. Now, it can be verified from Eq. (10) and (11) directly that

$$\epsilon_\alpha^{\text{eff}} \epsilon_\beta^{\text{eff}} = (\epsilon^B)^2 \text{ if } \epsilon_\alpha^A \epsilon_\beta^A = (\epsilon^B)^2. \quad (12)$$

Therefore, the MG formula for the effective medium of anisotropic circular cylinders in the small filling fraction limit is a special case of our central theorem Eq. (8). On the other hand, if we fix the anisotropy factor  $\gamma_A$  (defined as the ratio between the larger and the smaller principal index) of the cylinder and we vary the product  $\epsilon_\alpha^A \epsilon_\beta^A$  or  $\epsilon^B$ , we can prove from Eq. (10) and (11) directly that

$$\frac{\gamma^{\text{eff}} - 1}{\gamma^{\text{eff}} + 1} \leq f \frac{\gamma_A - 1}{\gamma_A + 1}. \quad (13)$$

with equality happens at the condition specified by Eq. (12).

## Appendix B: Effective medium for anisotropic periodically stratified medium

For a periodically stratified medium consisting of two layers A and B in a unit cell, we can specify the permittivity tensors of the two layers as

$$\boldsymbol{\varepsilon}^I = \begin{pmatrix} \varepsilon_{xx}^I & \varepsilon_{xy}^I \\ \varepsilon_{xy}^I & \varepsilon_{yy}^I \end{pmatrix} = R(\theta^I) \begin{pmatrix} \varepsilon_\alpha^I & 0 \\ 0 & \varepsilon_\beta^I \end{pmatrix} R(\theta^I)^T. \quad (14)$$

where  $I = A$  or  $B$ ,  $\varepsilon_\alpha^I$  and  $\varepsilon_\beta^I$  are the principal elements of permittivity tensor, and the rotation matrix is

$$R(\theta^I) = \begin{pmatrix} \cos \theta^I & -\sin \theta^I \\ \sin \theta^I & \cos \theta^I \end{pmatrix}. \quad (15)$$

in which  $\theta^I$  denotes the orientation of the optical axes of the two layers with respect to the x-axis, superscript “T” represents transpose of a matrix. Then we can write the constitutive relation for each layer as

$$\begin{pmatrix} D_x^I \\ D_y^I \end{pmatrix} = \boldsymbol{\varepsilon}^I \cdot \begin{pmatrix} E_x^I \\ E_y^I \end{pmatrix} = \begin{pmatrix} \varepsilon_{xx}^I & \varepsilon_{xy}^I \\ \varepsilon_{xy}^I & \varepsilon_{yy}^I \end{pmatrix} \begin{pmatrix} E_x^I \\ E_y^I \end{pmatrix}. \quad (16)$$

Considering the layers are stacked along the y-direction so that  $E_x$  and  $D_y$  are continuous across the boundary between A- and B-layer. Together with the fact that they vary so slowly within each layer in the long wavelength limit, we can safely regard them as constants throughout the whole unit cell, i.e.

$$E_x^A = E_x^B = \langle E_x \rangle, \quad D_y^A = D_y^B = \langle D_y \rangle. \quad (17)$$

where  $\langle \dots \rangle$  denotes the averaged fields. By putting Eq. (17) into (16), we can average the remaining two fields by

$$\begin{pmatrix} \langle D_x \rangle \\ \langle E_y \rangle \end{pmatrix} = f_A \begin{pmatrix} D_x^A \\ E_y^A \end{pmatrix} + f_B \begin{pmatrix} D_x^B \\ E_y^B \end{pmatrix} \quad (18)$$

with  $f_A$  ( $f_B$ ) being the filling fraction of the A (B) - layer and we obtain the effective constitutive relation ([11,12])

$$\begin{pmatrix} \langle D_x \rangle \\ \langle D_y \rangle \end{pmatrix} = \boldsymbol{\varepsilon}^{eff} \cdot \begin{pmatrix} \langle E_x \rangle \\ \langle E_y \rangle \end{pmatrix} = \begin{pmatrix} \varepsilon_{xx}^{eff} & \varepsilon_{xy}^{eff} \\ \varepsilon_{xy}^{eff} & \varepsilon_{yy}^{eff} \end{pmatrix} \begin{pmatrix} \langle E_x \rangle \\ \langle E_y \rangle \end{pmatrix} \quad (19)$$

where

$$\begin{aligned} \varepsilon_{xx}^{eff} &= f_A \varepsilon_{xx}^A + f_B \varepsilon_{xx}^B - \frac{f_A f_B (\varepsilon_{xy}^A - \varepsilon_{xy}^B)^2}{f_B \varepsilon_{yy}^A + f_A \varepsilon_{yy}^B}, \\ \frac{\varepsilon_{xy}^{eff}}{\varepsilon_{yy}^{eff}} &= f_A \frac{\varepsilon_{xy}^A}{\varepsilon_{yy}^A} + f_B \frac{\varepsilon_{xy}^B}{\varepsilon_{yy}^B}, \\ \frac{1}{\varepsilon_{yy}^{eff}} &= \frac{f_A}{\varepsilon_{yy}^A} + \frac{f_B}{\varepsilon_{yy}^B} \end{aligned} \quad (20)$$

hold for the bilayer system. Now it can be verified from Eq. (20) that

$$\det \boldsymbol{\varepsilon}^{eff} = \det \boldsymbol{\varepsilon}^A = \det \boldsymbol{\varepsilon}^B \text{ if } \varepsilon_\alpha^A \varepsilon_\beta^A = \varepsilon_\alpha^B \varepsilon_\beta^B \quad (21)$$

which is a special case of our central theorem Eq. (8). On the other hand, we can define anisotropy factor  $\gamma$  as the ratio between the larger and smaller principal index. It is related to the permittivity  $\boldsymbol{\varepsilon}$  tensor by

$$\gamma + \frac{1}{\gamma} = \frac{\text{Tr}(\boldsymbol{\varepsilon})}{\sqrt{\det \boldsymbol{\varepsilon}}} \quad (22)$$

Then, we fix the anisotropy factors  $\gamma_A$  and  $\gamma_B$  while we vary the product  $\varepsilon_\alpha^A \varepsilon_\beta^A$  or  $\varepsilon_\alpha^B \varepsilon_\beta^B$ , we can prove by extremizing Eq. (22) that  $\gamma^{\text{eff}}$  is at local maxima or local minima at the condition specified by Eq. (21).

### Acknowledgment

The work is supported by the National Natural Science Foundation of China (grant no.11104235) from Shenzhen Research Institute, City University of Hong Kong and the matching fund from Shenzhen government. SG acknowledges funding from European Research Council (grant no. 279673).